Magnetic-field-induced optical transmittance in colloidal suspensions

James E. Martin, Kimberly M. Hill, and Chris P. Tigges
Sandia National Laboratories, Albuquerque, New Mexico 87185
(Received 22 September 1998)

Through simulation and experiment we demonstrate that when a magnetic field is applied to a suspension of magnetic particles, the optical attenuation length along the direction of the field increases dramatically, due to the formation of chainlike structures that allow the transmission of light between the strongly absorbing particles. This phenomenon is interesting for two reasons; first, there might be practical applications for this effect, such as optical-fiber-based magnetic field sensors, and second, measuring the time evolution of the optical attenuation length enables us to determine the kinetics of structure formation, which can be compared to the predictions of simulation and theory. In agreement with both simulation and theory, the optical attenuation length increases as a power of time, but much less light is actually transmitted than expected, especially at higher particle concentrations. We conclude that particle roughness, which is not included in either theory or simulation, plays a significant role in structural development, by pinning structures into local minima. [S1063-651X(99)05405-7]

PACS number(s): 83.80.Gv, 82.70.Dd, 83.50.Pk

INTRODUCTION

Motivation. When a uniaxial electric or magnetic field is applied to colloidal suspensions having a sufficient permittivity or permeability mismatch, the particles will polarize and interact, causing them to chain along field lines and form complex columnlike and sheetlike structures. The concomitant change in the suspension rheology, which changes from a Newtonian liquid to a viscous, shear thinning fluid, is a subject of great interest because of the many possible industrial applications for field-controllable fluids, such as clutches, hydraulic valves, and dampers [1,2]. However, even in the quiescent state these fluids might have useful properties, since the induced structures can cause significant anisotropies in the fluid permittivity, conductivity, and optical transmittance [3]. In this paper we use experiment and simulations to examine the effect of the magnetic-field-induced optical transmittance in a strongly absorbing, nonscattering suspension of black magnetic particles. Studying the field-induced optical transmittance is interesting for two reasons. First, it is possible that this effect might be useful in certain applications, such as magnetic field sensors, and second, it couples to the kinetics of coarsening in induced dipolar fluids.

Experimental background. When a field is applied to an active colloidal suspension, anisotropic structures start to evolve, as exemplified by the simulation data in Fig. 1. Light scattering studies on a colloidal silica fluid structured by an electric field demonstrate that the emerging structures exhibit a well defined characteristic length, in the plane orthogonal to the applied field, that steadily increases as roughly the square root of time [4]. This behavior is somewhat analogous to the spinodal decomposition of a binary fluid and so this process is referred to as coarsening. By definition, light scattering measures the coarsening, or correlation, length but it is not obvious that other physical measurements couple strongly to this length.

In large scale dynamical simulations of field-structured suspensions, we have been able to compute a variety of physical properties from the structures generated [3,5]. Many of these, such as the anisotropic permittivity and conductivity, are strongly affected by chain formation, but do not couple to the correlation length and thus are insensitive to coarsening. For example, the conductivity of field-structured suspensions of conducting particles reaches essentially a plateau value shortly after chain formation. The permittivity of field-structured suspensions of dielectric particles behaves similarly. In fact, for some time we were unable to find any physical property that coupled directly to the correlation length, until we decided to compute the optical attenuation length [3]. The attenuation length shows a slow, power-law increase in time, with an exponent close to that obtained for the correlation length obtained from light scattering measurements, at least at low particle concentrations, suggesting a proportionality between these length scales.

Studying the optical attenuation length has two advantages over studying the correlation length. First, we have not been successful in obtaining the correlation length in the plane transverse to the field with great accuracy from the simulation data. Second, measurements of the evolution of the structure factor (the Fourier transform of the pair correlation function) must be done with light scattering, since both x rays and neutrons lack the required spatial and temporal resolution (with a Bonse-Hart x-ray scattering geometry the spatial resolution is adequate, but the temporal resolution is not, even on a synchrotron beam line) [6]. Light scattering measurements require optically transparent suspensions, and although we have been able to make measurements on optically transparent suspensions of smooth, dielectric spherical silica colloids, using an electric field to induce structure, the technique is not generally applicable [4]. The optical transmittance measurements described here on absorbing magnetic suspensions confirm the results of those light scattering experiments, but demonstrate more complex effects, such as the role of Brownian motion and particle roughness.

The connection of the optical attenuation length to the correlation length measured in scattering is not trivial, but

 ©1999 The American Physical Society

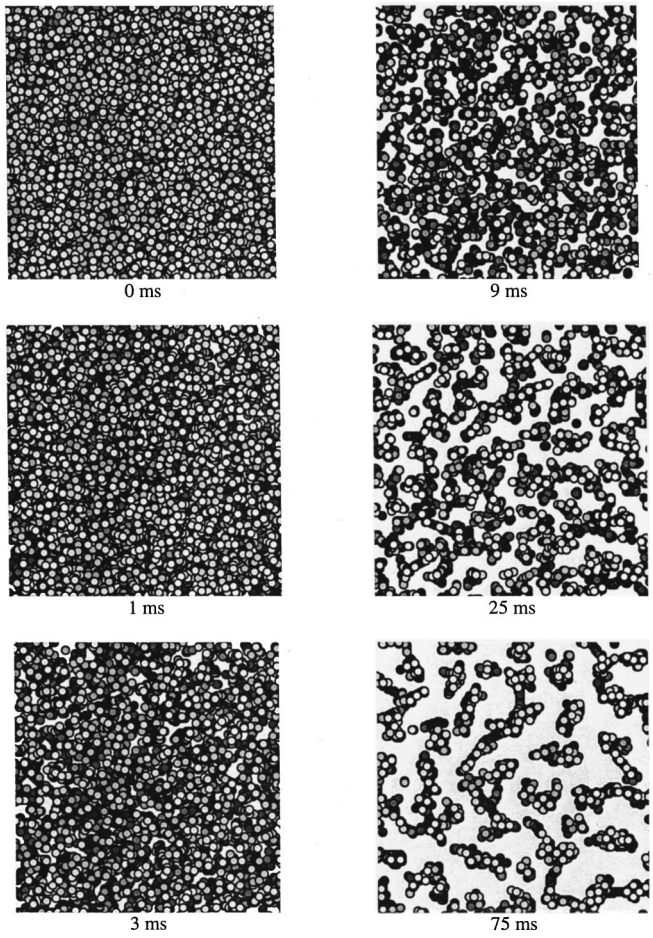

FIG. 1. Simulation results viewed along the direction of the applied field illustrate the evolution of the transmittance with coarsening time for an athermally structured 10 vol. % sample.

the optical attenuation length would be proportional to the correlation length if coarsening in these systems does not change the structure factor, apart from a change in scale. This scaling of the structure factor has been demonstrated in isotropic spinodal systems [7], and in the aforementioned light scattering measurements from an index-matched colloidal silica fluid structured by an electric field we were able to measure the correlation length both parallel and perpendicular to the applied field, and found that these lengths are indeed proportional to each other, with the correlation length parallel to the field about 10 times that perpendicular to the field. This scaling of the anisotropic structure factor is compelling enough that the evolution of the optical attenuation length can be compared to the evolution of the correlation length predicted from theory. To compare the attenuation length to simulations no assumptions are needed because we actually directly compute the optical attenuation length.

An intuitive understanding of the relation of optical attenuation to coarsening can be obtained from Fig. 1, which shows simulation results for an athermally structured 10% sample at selected coarsening times. From these views parallel to the field axis, one can see that as the particles coalesce into columns correlations propagate along the z axis, due to the tendency of chains to follow field lines. As these correlations increase, the structures transmit more light through the sample in the direction parallel to the magnetic field. At 75 ms the system is highly correlated in the direction parallel to the z axis, and the optical transmittance is high.

There have been some related optical studies reported in the literature. Lui *et al.* [8] studied the equilibrium optical transmittance, as a function of applied magnetic field, through a superparamagnetic ferrofluid emulsion of 0.3 μm kerosene particles containing 9 nm diameter iron oxide particles. These measurements were used to determine various critical fields thought to demarcate boundaries in a structural phase diagram. These measurements were not time resolved, however, and the droplets were too small to be close to the geometric optical limit, so the coarsening kinetics was not addressed in this study. Ginder *et al.* [9] made some interesting *diffuse* optical transmittance studies of a commercial electrorheological fluid consisting of 0.7 mm diameter poly(methacrylic acid) particles confined between transparent indium tin oxide electrodes. Time resolved studies demonstrated a field-squared dependence of the characteristic structure formation time, but extraction of the solution correlation length was not a goal in this work, due to the complex relation of the multiple scattering process to structure, which would require the solution of an ill-conditioned inverse transform problem. A number of optical studies have been done on the field-induced turbidity of weakly scattering particles chained by an electric field [10–12]. In these systems the *increase* in turbidity, and the concomitant *decrease* in light transmittance, is attributed to the formation of strongly scattering chainlike structures. The scattered intensity of a solution of such structures increases in proportion to the aggregation number at fixed solution concentration.

Theoretical background. In the current understanding of coarsening in induced dipolar fluids a distinction is made between magnetic and electrostatic structuring, due to the difference in the boundary conditions at the confining surfaces normal to the applied field, which in turn are due to the fact that electric monopoles exist, whereas magnetic monopoles apparently do not. In the electrostatic case, these surfaces are typically conducting electrodes that do not permit a tangential electric field, whereas in the magnetic case these surfaces can be low permeability, diamagnetic materials such as glass, so that a tangential magnetic field is possible, or can be high permeability ferrous materials, which reduce the tangential magnetic field. In our experiments, chains of magnetic particles simply terminate at the glass sample cell, leaving an effective ''magnetic capping charge'' that creates a long range, repulsive interaction between chains or columns. Calculations show that tapering the ends of the columns to make ellipsoidal columns minimizes the energy of these magnetic structures, whose width is dependent on the sample dimension along the field [13,14]. In the electrostatic case [14], the boundary conditions create image charges, which effectively eliminate the capping charge, and also reduce the interaction between chains, as we will now discuss.

One current theoretical view of coarsening in systems structured by an external field postulates a clean temporal separation of two processes: chain formation and column formation. In this view particles first chain along field lines to span the cell, then aggregate into columns, which then aggregate into thicker columns, *ad infinitum* [4,14]. Computing the chain-chain interaction in the electrostatic case is a

delicate issue, because image charges in the conducting electrodes virtually eliminate interactions between perfect field-aligned chains separated by more than a particle diameter or so. However, it has been shown that thermal fluctuations in the chains can create a large electrostatic interaction, despite the image charges, so that temperature can actually drive coarsening. Pursuing this line of reasoning leads to the prediction of a roughly root time growth of the correlation length in the plane transverse to the field. The coarsening kinetics predicted by this *thermally driven coarsening* model is supported by light scattering measurements [4], although the key prediction, that of the temperature dependence, is not easily amenable to experimental verification, since many other factors, such as the conductivity and permittivity contrast, have complex temperature dependencies themselves.

The role of thermal fluctuations is to create disorder that breaks the symmetry of perfect chains, but there are other sources of disorder one can envisage, including particle polydispersity and the possibility that *perfect* chains never actually exist, only highly defective chainlike structures. This later view is supported by dynamical computer simulations we have conducted on large scale systems containing 10 000 particles [3]. Over the concentration range of 5–60 vol. % we have not been able to find a system that exhibits perfect chains that span the electrodes, regardless of the system temperature. Instead, the evolution of highly defective chainlike structures occurs, and these defective structures have large dipolar interactions, regardless of the presence of image charges. We call this *defect-driven coarsening*. The importance of defects in driving coarsening is clearly demonstrated in simulations where the temperature is set to zero. In this case thermally driven coarsening should not occur, yet in fact coarsening proceeds at essentially the same rate as when thermal fluctuations are strong. Perversely, these athermal simulations show the same nearly root-time growth kinetics predicted by the thermal fluctuation model—an unfortunate circumstance for the experimentalist, since this implies that the agreement between light scattering measurements and the thermally driven coarsening model is not a compelling validation of this theory, nor of the computer simulations for that matter, but disagreement with measurement could rule out both.

In the following we describe our simulation and experimental methods and present the results of these. We investigate the complex role temperature can play, and conduct experiments that elucidate the importance of particle friction. Finally, we discuss possible applications of optical transmittance in field-structured materials.

EXPERIMENTAL

Simulations. We have already reported athermal simulation studies of structure formation in induced dipolar fluids, including the time evolution of the optical attenuation length [3]. In this paper these studies are extended to include Brownian motion, which can have a large influence. Briefly, in these Langevin dynamics simulations the particles are essentially hard spheres with induced dipolar interactions, Stokes friction against the solvent, and Brownian motion. The results presented here are obtained from a simulation method developed to predict the evolution of large, $N = 10\,000$ particle systems over short times (in general, $\leqslant 150$ dimensionless time units). This method has time complexity $O(N)$, but gives results that are indistinguishable from a separate, more direct $O(N^2)$ simulation developed to predict the evolution of smaller systems over longer times. In most of the simulations cyclic boundary conditions are used in all directions, but in some simulations the cyclic boundary conditions were dropped along the z axis, which is the direction of the applied field, and thus should be more representative of magnetic systems, due to the presence of a capping charge. The size of the simulations led to structures whose scale of coarseness was much smaller than the simulation volume, minimizing the effect of the cyclic boundary conditions.

To describe our simulation we start with the equation of motion for the ith sphere,

$$m\mathbf{a}_i = \mathbf{F}_h(\mathbf{v}_i) + \sum_{j\neq i} \mathbf{F}_{\rm hs}(r_{ij}) + \sum_{j\neq i} \mathbf{F}_d(r_{ij},\theta_{ij}) + \mathbf{F}_B, \quad (1)$$

where $\mathbf{F}_h$ is the hydrodynamic Stokes force, $\mathbf{F}_{\rm hs}$ is the hard sphere force, $\mathbf{F}_d$ is the dipolar force, and $\mathbf{F}_B$ is the Brownian force, discussed below. r_{ij} is the distance between the centers of spheres i and j, and θ_{ij} is the angle between the line of centers of spheres i and j and the direction of the applied field. The inertial term is small compared to the other forces, and is neglected, so that we integrate a system of first order differential equations.

The Stokes force on a sphere of radius a is $\mathbf{F}_h(\mathbf{v}) = -6\pi\eta_0 a\mathbf{v}$ where η_0 is the solvent viscosity and $\mathbf{v}$ is the sphere velocity. The spheres are modeled as nearly hard spheres, with a repulsive force dependent on the gap between spheres, $\mathbf{F}_{\rm hs}(r_{ij}) = A/(r_{ij} - cd)^{\alpha}$, where d is the sphere diameter and $\alpha = 7$ and $c = 0.97$ are constants. The dipolar interaction [2] between two spheres whose center of mass separation vector is of length r and inclined at an angle θ to the applied field $\mathbf{E}_0$ is

$$\mathbf{F}_d(r_{ij},\theta_{ij}) = -C\left(\frac{d}{r}\right)^4 [(3\cos^2\theta - 1)\hat{\mathbf{r}} + \sin 2\theta\hat{\boldsymbol{\theta}}]. \quad (2)$$

Note that although the radial component of the dipolar force is attractive only when $\theta < 54.7°$, the tangential component of the force will always lead to chaining in a system with finite noise.

For a system of dielectric particles in an electric field

$$C = \frac{3}{16}\frac{p^2}{4\pi a^4 \varepsilon_0 \kappa_c},$$

where the particle dipole moment is $\mathbf{p} = 4\pi a^3 \varepsilon_0 \kappa_c \beta \mathbf{E}_0$, the dielectric contrast factor is $\beta = (\kappa_p - \kappa_c)/(\kappa_p + 2\kappa_c)$ in terms of the dielectric constants of the particle and continuous (liquid) phases, and $\varepsilon_0 = 8.854 \times 10^{-12}$ F/m is the vacuum permittivity. Combining gives the well-known result $C = (3\pi/4)\varepsilon_0 \kappa_c a^2 \beta^2 E_0^2$.

For a system of magnetic particles in a magnetic field [15],

$$C = \frac{3}{16}\frac{\mu_0 \kappa_{\mu,c} m^2}{4\pi a^4}.$$

For paramagnetic (or diamagnetic) particles the magnetic moment is $\mathbf{m}=4\pi a^3\beta_\mu \mathbf{H}_0$, in terms of the magnetic contrast factor is $\beta_\mu=(\kappa_{\mu,p}-\kappa_{\mu,c})/(\kappa_{\mu,p}+2\kappa_{\mu,c})$, where $\kappa_{\mu,c}$ is the relative permeability (to the vacuum) of the continuous (liquid) phase, $\kappa_{\mu,p}$ is the relative permeability of the particles, and $\mu_0=4\pi\times10^{-7}$ H/m is the vacuum permeability. Combining these gives an expression completely analogous to the dielectric case $C=(3\pi/4)\mu_0\kappa_{\mu,c}a^2\beta_\mu^2H_0^2$. (Note in the magnetic case that although the expression for the particle interaction is perfectly analogous to the electric case, the expression for the magnetic dipole is not, due to the fact that the magnetization has the units of the magnetic field **H**, whereas the polarization has the units of the displacement field **D**.)

If this system consists of ferromagnetic particles then the expression for the magnetic moment deserves further consideration. The particles we use in our experiments are easily dispersed, indicating that they are unpoled, so that a typical particle consists of many domains whose magnetization vectors are essentially randomly aligned. When such particles are exposed to a saturating magnetic field $\mathbf{H}_s$ the domain walls move to create a magnetic dipole moment that is roughly $\mathbf{m}_s=(4\pi/3)a^3\mathbf{M}_s$, where $\mathbf{M}_s$ is the saturation magnetization along the easy axis of the magnetic material. After this poling field is turned off, the moment will decay to $\mathbf{m}_r=(4\pi/3)a^3\mathbf{M}_r$, where $\mathbf{M}_r$ is the remnant magnetization, and this moment can be much larger than that induced on a paramagnetic particle $\mathbf{m}=4\pi a^3\beta_\mu\mathbf{H}_0$. When a poled magnetic particle is subsequently exposed to a small magnetic field, the energy will be $\mu_0\mathbf{m}_r\cdot\mathbf{H}_0$ and a standard statistical mechanical calculation shows that the average moment along the z axis will be given by the Langevin-Debye function [16]

$$m_z=m_r\left[\coth y-\frac{1}{y}\right],$$

where

$$y=\frac{\mu_0 m_r H_0}{k_B T}.$$

For small magnetic fields, where $y\ll1$ this gives $m_z\cong\mu_0 m_r^2H_0/3k_BT$, and for large magnetic fields, where $y\gg1$, $m_z=m_r$.

It is instructive to estimate the paramagnetic and ferromagnetic moments we might expect for our particles. The minor (low field) hysteresis loops of ferromagnetic materials can be closely approximated as a paramagnetic response with a relative permeability on the order of $\kappa_{\mu,p}\approx10^4$. Because the relative permeability of the liquid phase is essentially 1, this gives $\beta_\mu\approx1$. For a typical magnetic field produced by our solenoid of $H_0\cong4\times10^3\,\mathrm{Am}^{-1}$ (50 Oe), and a particle radius of 1 μm, this gives a dipole moment $m\cong5.0\times10^{-14}\,\mathrm{Am}^2$. The particles used in the experiments described in this paper are made of carbonyl Fe, which has a very small remnance, and Fe_3O_4, which has a remnant magnetic induction of $B_r\cong0.2100$ T (2100 G) according to the manufacturer. The remnant magnetization is thus $M_r=B_r/\mu_0\cong1.7\times10^5\,\mathrm{Am}^{-1}$ and the remnant magnetic dipole moment will be an order of magnitude larger than in the paramagnetic case $m_r=7.0\times10^{-13}\,\mathrm{Am}^2$. The interaction energy in the applied field will be $\mu_0 m_r H_0=3.5\times10^{-15}$ J, and because the thermal energy at room temperature is $k_BT=4.1\times10^{-21}$, the Langevin-Debye variable $y\gg1$, and poled particles would be completely aligned with this applied field, and would even align with the earth's magnetic field (0.7 Oe). Furthermore, the energy required to separate two such poled ferromagnetic particles in contact is $m^2\mu_0/16\pi a^3=1.2\times10^{-14}$ J, which is vastly in excess of the thermal energy, so that such particles would not disperse well (the particle radius would have to be decreased to about 7 nm for the contact energy to equal the thermal energy). Because the particles we use are easily dispersed, we conclude that they are initially unpoled, and because the fields we apply are far beneath the saturation field we can think of the particles as essentially superparamagnetic.

Time scale. In the absence of Brownian motion the strength of the dipolar interactions alters only the coarsening time scale, not the structural evolution. The dimensionless numerical equation of motion is thus of the form $\Delta u=\Delta s f(r,\theta)$, where the dimensionless length $\Delta u=\Delta r/2a$. For the magnetic case the dimensionless time $\Delta s=\Delta t\mu_0\kappa_{\mu,c}\beta_\mu^2H_0^2/16\eta_0$. For a suspending liquid with a viscosity of 1 cp, an applied field of $H_0=11.3\times10^3$ A/m (142 Oe), $\kappa_{\mu,c}=1$ and $\beta_\mu=1$, $\Delta s\cong\Delta t\times10^3$, so under these conditions one dimensionless time unit is about a millisecond.

For the electric field case the dimensionless time $\Delta s=\Delta t\varepsilon_0\kappa_c\beta^2E_0^2/16\eta_0$. For a viscosity of 1 cp, an applied field of 1.0 kV/mm, and $\varepsilon_c\beta^2=2$, $\Delta s\cong\Delta t\times10^3$, so one dimensionless time unit is about a millisecond. This time conversion is used in all plots in this paper. Note that this implies that the coarsening kinetics is independent of ball size.

Brownian motion. The Brownian force requires some discussion. There are a number of problems one encounters in implementing Brownian motion into a simulation where one is integrating a first order differential equation. A short discussion of the manner in which we chose to do this is useful. This is not the only possible approach, but it is a method that allows one to incorporate the effect of particle inertia without resorting to a second order differential equation.

The equation of motion of a Brownian particle is [17]

$$m\dot{\mathbf{v}}=-\zeta\mathbf{v}+\mathbf{F}_B(t), \tag{3}$$

where $\mathbf{v}$ is the particle velocity, m is the particle mass, and $\zeta=6\pi\mu_0 a$ is the friction coefficient of a particle of radius a against a liquid of viscosity μ_0. $\mathbf{F}_B(t)$ is a stochastic force that is generally considered to have a time correlation function that is a delta function. The time correlation function of the diffusing particle is

$$\langle\mathbf{v}(0)\cdot\mathbf{v}(t)\rangle=\frac{3k_BT}{m}e^{-t/\tau}, \tag{4}$$

where the relaxation time is $\tau=m/\zeta$. Using the Kubo relation [17]

$$D=\frac{1}{3}\int_0^\infty\langle\mathbf{v}(0)\cdot\mathbf{v}(t)\rangle dt \tag{5}$$

then gives the Stokes-Einstein relation for the translational diffusion coefficient $D=k_BT/\zeta$. Thus it is the persistence of

motion of a particle acted upon by a stochastic force that is responsible for a finite diffusion coefficient. In some sense the situation is very subtle; the diffusion coefficient is indeed independent of the particle mass, but the relaxation time is proportional to the mass, and the amplitude of the velocity autocorrelation function is inversely proportional to the mass. Thus as the particle mass goes to zero, the force amplitude diverges.

The characteristic relaxation time for a 1 μm diameter silica sphere in water is 5.5×10^{-7} s, but we would expect an applied field of 1.0 kV/mm to structure silica spheres in such a solution on millisecond time scales. In our previous simulation work we set the discrete time step to a maximum of 2.0×10^{-5} s, so the natural time scale for Brownian motion is strongly decoupled from the time scale we wish to investigate. Thus a completely physical simulation of field structuring with Brownian motion is not feasible and a practical method must be found.

We start with the first order differential equation $\zeta\mathbf{v}=\mathbf{F}_B(t)$, obtained by dropping the inertial term. If $\mathbf{F}_B(t)$ is considered to be a stochastic force with a delta function time correlation function, then the diffusion coefficient of a particle will now depend on the discrete time step used to solve the equation. For example, consider the simple one-dimensional case where $F_B(t)=f_B s_i$, and s_i is a simple uncorrelated random variable that is either ±1 during the ith time step. Then during the time Δt the particle will move a distance $\Delta x=(f_B/\zeta)\Delta t$. Over a total time t the number of steps will be $N=t/\Delta t$ and from the theory of random walks the mean square displacement will be $\langle x^2\rangle=N\Delta x^2=(f_B/\zeta)^2 t\Delta t$. Thus the diffusion coefficient $D=\frac{1}{2}(f_B/\zeta)^2\Delta t$ has an unphysical dependence on the discrete time step. A simple way to handle this is to scale the amplitude of the Brownian force by $f_B\propto1/\sqrt{\Delta t}$. However, this leads to divergent force amplitudes that can create stability problems when two ''hard'' spheres are nearly in contact.

To avoid stability problems we have taken a different approach. Let us write the Brownian force as $\mathbf{F}_B(t)=f_B\mathbf{R}_v$, where $\mathbf{R}_v$ is a time-correlated random variable. Using the Kubo relation we then have $D=(f_B/\zeta)^2\int_0^\infty\langle R_{v,x}(0)R_{v,x}(t)\rangle dt$, where we have used the isotropy of space to obtain $\langle\mathbf{R}_v(0)\cdot\mathbf{R}_v(t)\rangle=3\langle R_{v,x}(0)R_{v,x}(t)\rangle$. If our time correlated variable is normalized such that $\langle R_{v,x}(0)R_{v,x}(t)\rangle=1$, then the relaxation time is $\tau=\int_0^\infty\langle R_{v,x}(0)R_{v,x}(t)\rangle dt$, and $D=(f_B/\zeta)^2\tau$. The amplitude of the Brownian force is now $f_B^2=K_BT\zeta/\tau$, and so can be controlled by a judicious selection of τ.

To construct the correlated random variable we start with the primitive uncorrelated random variable s_i, with $\langle s_i s_j\rangle=\delta_{ij}$. Define the function $\Gamma_i=(1-\varepsilon)\Gamma_{i-1}+\varepsilon s_i$ and note that by a straightforward calculation the exponential correlation $\langle\Gamma_i\Gamma_{i+k}\rangle=[\varepsilon/(2-\varepsilon)](1-\varepsilon)^k$ is obtained. If we let $R_i=[(2-\varepsilon)/\varepsilon]^{1/2}\Gamma_i$ then $\langle R_i R_{i+k}\rangle=(1-\varepsilon)^k$ and $\tau=1/\varepsilon$. In practice, the correlation time is chosen to be larger than the maximum discrete time step of 2 μs, but smaller than the ms time scale of structural evolution. We chose 10 μs. The computed diffusive motion is shown in Fig. 2, where the crossover from ballistic to diffusive motion can be clearly seen. Thus the effect of particle inertial on diffusion is obtained without resorting to a second-order differential equation.

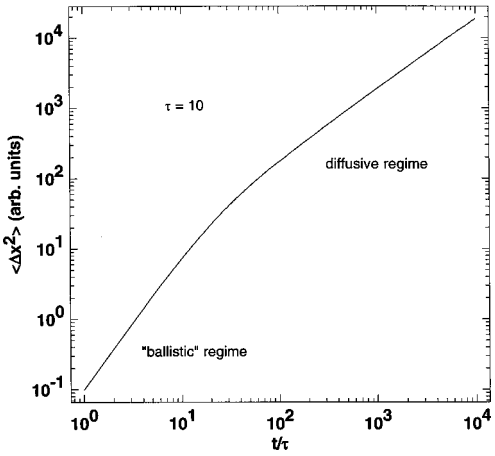

FIG. 2. Crossover from the ''pseudoballistic'' to Brownian regimes for a massless particle subjected to a correlated fluctuating force.

Temperature scale. In the dimensionless equation we solve, the Brownian motion enters as $J\mathbf{R}_v$ where the dimensionless constant $J=2f_B/f_c$ and $f_c=3\pi a^2\mu_0\kappa_{\mu,c}\beta_\mu^2H_0^2/2$ is the contact force between two balls aligned along the z axis in a uniaxial field. We refer to the value of J throughout this paper, but it is more conventional to talk in terms of $\lambda^{-1}=k_BT/\pi\mu_0\kappa_{\mu,c}\beta_\mu^2H_0^2a^3$. The relation between these variables is $\lambda^{-2}=(9D\tau/a^2)J^2$, and noting that the time it takes a particle to diffuse its own radius a is $\tau_D=(a^2/6D)$ we obtain $\lambda^{-2}=(3\tau/2\tau_D)J^2$.

Computation of the transmittance. The optical transmittance through the simulated structures was computed in the geometrical optics limit. The geometric transmission area is calculated by keeping a set of lists of projected ball boundaries within subregions of the total projection region. The subregions form a compact set of rectangles with a union equal to the total projected area and a size calculated to insure a simple projected boundary within each subregion. The subregions are classified as interior (zero transmission), partial (partial transmission), and exterior (complete transmission). The transmission area for interior and exterior subregions is trivial. The transmission area of a subregion classified as partially transmitting is determined by examining the boundary list (ball coordinates contributing to the transmission boundary) generated for that subregion. The relevant area corresponds to interior to the subregion that is also exterior to the calculated boundary.

Optical transmittance. For the optical transmittance studies we chose to use magnetic particles in a magnetic field, rather than dielectric particles in an electric field, for two reasons. First, a solenoid allows measurement of the light transmitted parallel to the applied field, without the problems of light reflection one would have with conducting indium tin oxide coated electrodes. Second, black magnetic particles, with high optical absorption, are easily obtained.

Sample preparation. Two types of magnetic particles were used for these experiments. Rough, submicron particles of Fe_3O_4 (Wright Industries) and relatively smooth carbonyl Fe particles made from reducing iron pentacarbonyl (Lord Corporation). These particles were suspended in a mixture of glycerin and 1,4 butanediol using 2 wt% Triton X-100 as a dispersant. The composition of this binary solvent was ad-

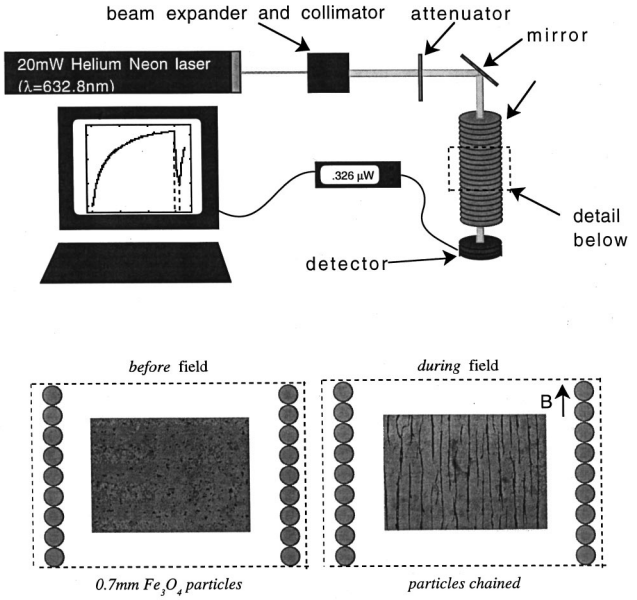

FIG. 3. Schematic of the experimental setup. The detail at the bottom shows actual images of the Fe_3O_4 particles before and after applying a magnetic field.

justed to achieve a viscosity of 300 cp, which was large enough to prevent sedimentation during the time it took to load the sample into the solenoid and also resulted in coarsening kinetics that were slow enough to measure with our experimental apparatus, but fast enough to complete the experiment before dinner. The particle concentration ranged from 1–5 wt. %, approximately 0.2–1 vol. %.

Transmittance measurements. The experimental apparatus is illustrated in Fig. 3. The particle suspension is contained in a transparent $10\times10\times1$ mm cell positioned in the center of a vertical solenoid and held in place by a black anodized aperture that serves both to remove stray light as well as to support the sample cell. The small dimension of the cell is normal to the axis of the solenoid and incident laser beam, so that the longest particle chains would be 1 mm, or approximately 1500 particle diameters. The axis of the solenoid is vertical to prevent column sedimentation. The current through the solenoid provides magnetic inductance fields ranging $B=0-6.0\times10^{-3}$ T (0–60 G).

The light source is a 20 mW helium-neon laser ($\lambda=632.8$ nm) directed through a beam expander and collimator, an aperture set at 5.5 mm, and a variable attenuator. The beam is expanded to sample a larger area of the particle suspension, and attenuated to insure measurements are made in the linear response regime of the photodiode detector. The beam is then reflected down the central axis of the solenoid to pass through the sample cell, and through the second aperture. The intensity of the transmitted beam is monitored with a Newport 818-uv silicon photodetector, connected via an IEEE parallel port to an Apple Quadra 950™ computer running an application written in LABVIEW™. The temperature is kept ambient with the help of a fan.

One issue is whether or not the transmitted light can be interpreted in the geometrical optics limit to a reasonable approximation, without considering the effects of multiple scattering and diffraction. If multiple scattering is an important effect, we would expect the transmitted light to contain a large depolarized component; in the strong multiple scattering limit the light would be thoroughly depolarized, so that 50% of the measured intensity would be transmitted through a polarizing filter orthogonal to the polarization of the incident beam. Over the range of particle concentrations considered in this study, less than 1% of the transmitted light is depolarized at the lowest concentration, and about 3% is depolarized at the highest concentration. Thus the effect of multiple scattering is small. The particles are sharp and clear under an optical microscope, so the effects of diffraction appear not to be significant either. In any case, our simplified treatment of the data must be viewed as approximate, but the disparity of the experimental data with the predictions of simulations is far too large for these effects to account for the difference.

Data analysis. Obtaining the optical transmittance from experimental data, where we only have the measured transmittance through the entire sample, is not as accurate as from simulation data, where the optical attenuation length can be obtained from a semilog plot of the optical transmittance against the sample thickness. For experimental data we must resort to curve fitting. The expected functional form of the transmittance we base on the simulation results, which indicate that the attenuation length L_t should be of the form

$$L_t=L_0(1+t/\tau_0)^{\beta}\cong L_0(t/\tau_0)^{\beta} \quad \text{for} \quad t\gg\tau_0, \tag{6}$$

where L_0, τ_0, and β are constants. According to Beer's law, $I_t/I_0\propto\exp(-L/L_t)$, so the transmittance $T=I_t/I_0$ takes the form

$$T=T_\infty/\exp(\tau/t)^{\beta}, \tag{7}$$

where $T_\infty=T(t\to\infty)$; $\tau=\tau_0(L/L_0)^{(1/\beta)}$ is the new time scale. Note that in order to obtain the exponent β from a semilog plot one must know T_∞.

SIMULATION RESULTS

The coarsening of systems of particles with induced magnetic and electric dipoles has been the much discussed in the literature. The principal difference between these cases is due to the boundary conditions at the confining surfaces perpendicular to the field. In the electric field case these surfaces are generally conducting electrodes that permit no tangential component of the field, and thus require image dipoles. Halsey and Toor [14] have pointed out that a field-aligned chain of perfectly monodisperse spheres that spans the gap between confining electrodes will create image dipoles in each electrode, which in turn will create image-image dipoles in the opposite electrode, *ad infinitum*, so that these finite real chains become equivalent electrically to infinitely long chains of dipoles. In effect, the capping charge is moved to infinity, with the consequence that the electric field decays exponentially rapidly in the plane normal to the chain. In magnetic systems the confining low permeability surfaces can have a tangential component of the magnetic field, image dipoles are thus irrelevant, and chains of magnetic dipoles are effectively terminated with a capping charge, so the ends of neighboring chains repel each other. An important consequence of this difference between electric and magnetic systems is in the structures that minimize the energy; for in-

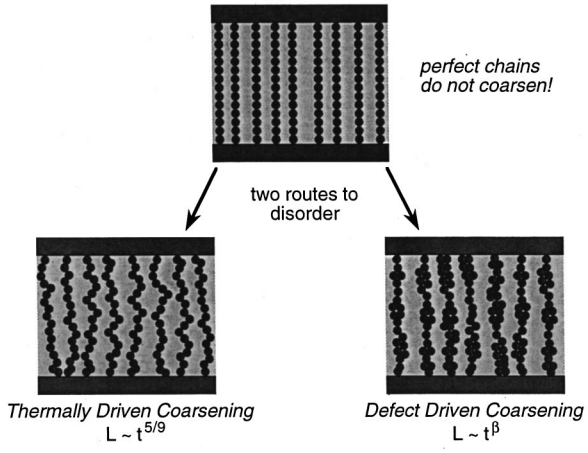

FIG. 4. Long range interactions between chains can be induced by disorder due to thermal fluctuations or defects.

duced electrical dipoles this is a body-centered tetragonal (bct) lattice, whereas the energy of magnetic dipoles is minimized by elliptical bct columns.

Coarsening and disorder. As mentioned in the Introduction, disorder in the form of thermal fluctuations can create an interaction between chains of perfect electric dipoles. The

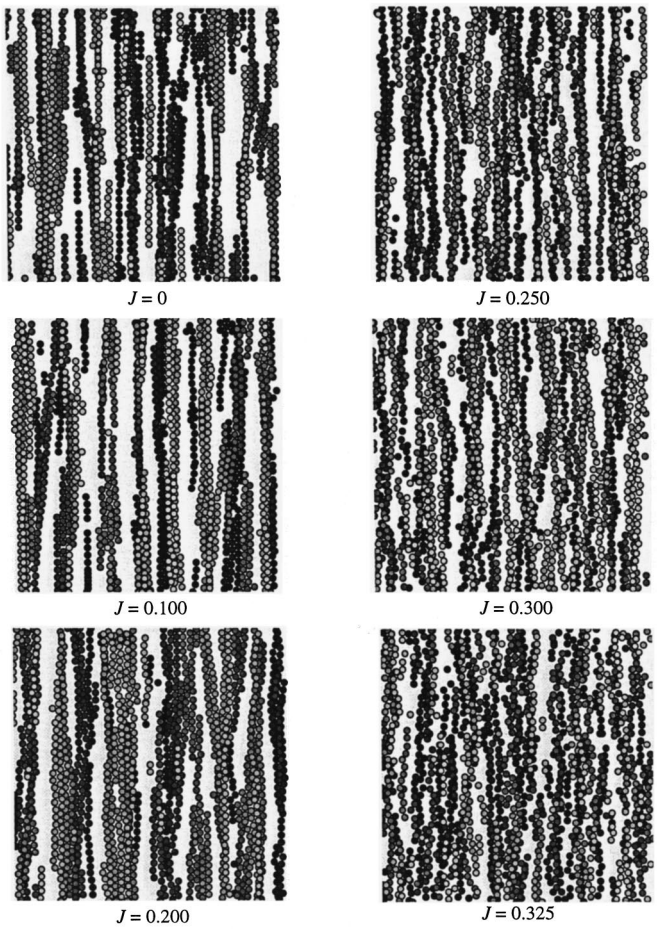

FIG. 5. Simulations show the development of highly defective chainlike structures at all reduced temperatures. These images are thin sections of a 10% sample viewed perpendicular to the field axis after 75 ms of coarsening.

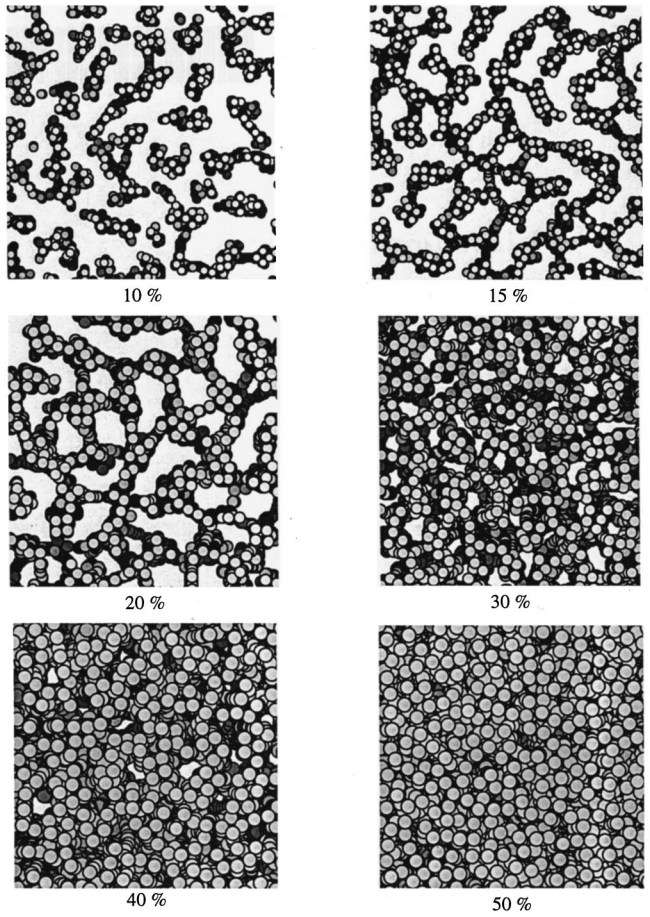

FIG. 6. Simulated structures, viewed parallel to the field, at various particle concentrations after 75 ms of coarsening.

way in which thermal fluctuations can lead to coarsening was initially described by Halsey *et al.* [14], and later modified in Martin *et al.* [4]. Fundamental to the model is the assumption that growth occurs in two stages: chain formation and column formation. In the chain formation stage, dipoles aggregate along field lines to form perfect chains that span the electrodes. These chains then aggregate to form columns, which then aggregate to form ever larger columns. This *thermally driven coarsening* model is based on viewing columns of dipoles are essentially one-dimensional solids that are therefore subject to strong thermal Landau-Peierls fluctuations [18] that give rise to long-range, power-law, chain-chain interactions. This thermal coarsening model leads to the power-law coarsening kinetics $L \sim t^{5/9}$, where L is the characteristic column separation, a prediction that is consistent with light scattering measurements [4], that give a coarsening exponent of 0.5 ± 0.1. The application of this model to systems of magnetic particles is not completely correct, due to the fact that these chains terminate magnetically at the bounding surfaces, and so have a residual ''capping charge'' at the ends. However, if one examines the field around a finite chain of dipoles, one finds that the field is extremely small near the chain, and then decays algebraically some distance away from the chain. In any case, our simulations indicate that the difference between magnetic and electric systems might be overemphasized in theories that pertain to idealized structures, as we will now discuss.

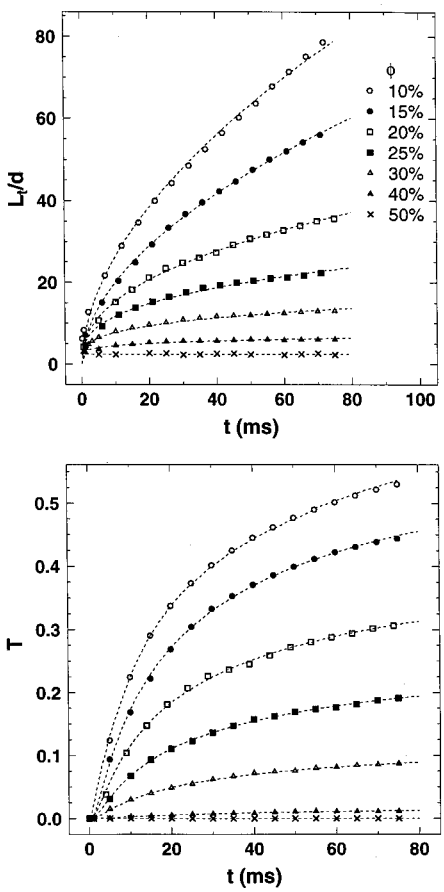

FIG. 7. Attenuation length and transmittance for athermal simulations at selected particle concentrations. The parameters for the fitting functions, Eqs. (6) and (7), are in Table I.

We have recently conducted large scale athermal and thermal simulations of structure formation in induced dipolar fluids, and have found that coarsening takes place even in the absence of thermal fluctuations [3,5]. We call this *defect-driven coarsening* because it arises from the many defective structures that grow in a dynamical simulation. In these simulations a decoupling of growth between chain formation and column formation is not found, but instead coarsening proceeds through the evolution of complex structures. For example, single balls or groups of balls might cling to the sides of columns, as illustrated in the bottom right hand corner of Fig. 4. In this case the columns interact even without thermal fluctuations. The addition of a single defect to a perfect chain in the form of a particle stuck to the side of the chain, creates a local field that is essentially equal to that of the individual dipole.

TABLE I. Optical transmittance fitting parameters for simulated athermal structures. (The values of β obtained from fitting L_t were used to fit the transmittance curves.)

ϕ	β	T_∞	τ
0.10	0.55	0.81	15.7
0.15	0.53	0.72	19.2
0.20	0.43	0.50	20.0
0.25	0.34	0.32	22.2
0.30	0.28	0.15	24.6
0.40	0.17	0.077	47.6
0.50	(0.002)	(6.2*e*-5)	(1.54)

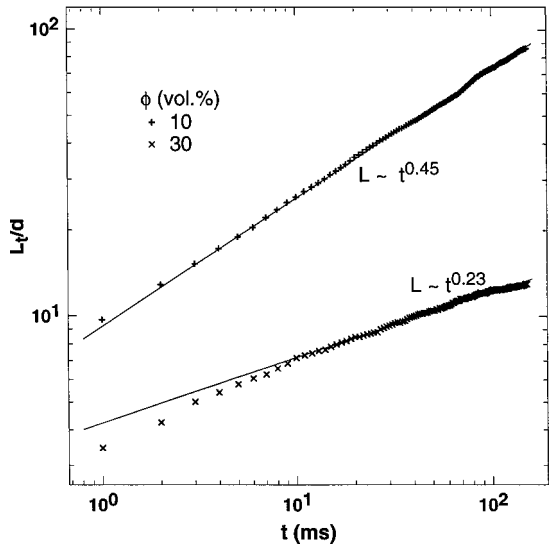

FIG. 8. The evolution of the optical attenuation length without cyclic boundary conditions along the field axis. Removing the boundary conditions forces chains into registration and creates a capping charge, yet seems to make little difference, due to the high occurrence of defects. The coarsening exponent at 10 vol. % is 0.55 with cyclic boundary conditions and 0.45 without. At 30 vol. % the respective exponents are 0.28 and 0.23.

These simulation studies, nor any others of which we are aware [19,20], have not yet revealed the existence of perfect spanning chains, at least over the concentration range we have investigated. Instead, the chains show defects at all temperatures, as can be seen in Fig. 5, which shows chaining in a 10 vol. % suspension at selected temperatures after 75 ms in an applied field. At the lowest temperatures shown, the columns are well aligned with the field, but contain many defects. As the temperature increases the number of structural defects decreases, and thermal fluctuations become an important component of the observed disorder in the system. These simulations have been performed with and without cyclic boundary conditions along the direction of the applied field, and the results are very similar. One would expect simulations with cyclic boundary conditions to be more representative of the electrostatic case and simulations without to be more representative of the magnetic case.

Compelling evidence that defects drive coarsening is given in Fig. 1, where coarsening is demonstrated in the absence of thermal fluctuations. The thermally driven coarsening model would predict no coarsening in this case, but coarsening clearly occurs. Thermal simulations indicate that temperature can have an effect on the manner and degree of the coarsening, but primarily by preventing trapping into local energy minima.

Athermal coarsening. Simulations of coarsening in the absence of thermal fluctuations yield the structures shown in Fig. 6, over the concentration range of 10–50 vol. %, after 75 ms. The fits of the attenuation length $L_t = L_0(t/\tau)^\beta$ and the transmittance $T = T_\infty/\exp(\tau_0/t)^\beta$ are in Fig. 7, and the fitting parameters are in Table I. At higher concentrations the coarsening exponent decreases, as does the asymptotic transmit-

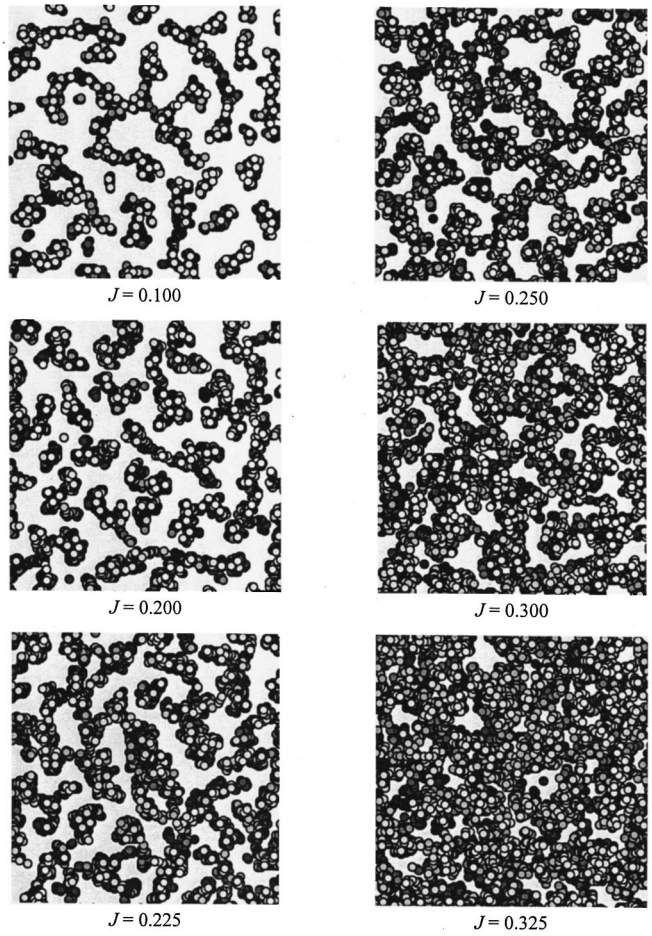

FIG. 9. Simulations illustrate how thermal fluctuations reduce the transmittance. These 10 vol. % structures are viewed along the field axis after 75 ms of coarsening.

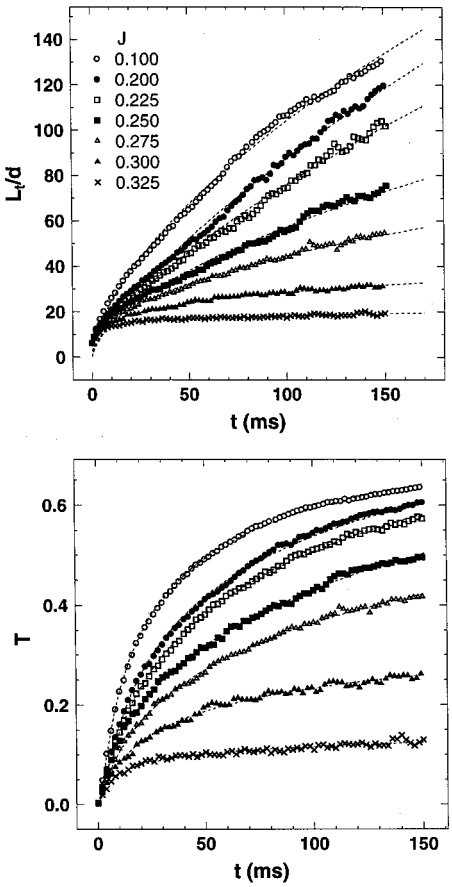

FIG. 10. The evolution of the optical attenuation length and transmittance as a function of time for 10 vol. % suspensions at selected reduced temperatures.

tance, although the fits of the 40 and 50 vol. % simulations are not meaningful, since the transmittance did not come close to T_∞ over the duration of the simulation. At these concentrations the computed optical transmittance is much smaller than expected, due to the slow dynamics of these congested systems.

At 10 vol. % the exponent for the optical attenuation length is approximately $\beta = 0.55$, coincidentally close to the prediction of the thermally driven coarsening model, and close to the root time dependence of the correlation length determined by light scattering measurements on electric-field-structured fluids. That these two coarsening mechanisms give essentially the same time dependence is reasonable, as both defect structures and thermal fluctuations give a long range, $1/r^4$ power-law interaction. Unfortunately, it is thus not possible to determine which model is relevant to experiments merely by measuring the rate of structural formation. However, an appropriately designed experiment has allowed us to verify the validity of the coarsening predictions in both theories, and has led to an appreciation of the importance of particle friction in experimental systems that consist of rough particles.

These athermal simulations were done with cyclic boundary conditions along the z axis, which both eliminates the capping charge, and the tendency for chains to be in registration near the surfaces normal to the field. We ran additional simulations without the cyclic boundary conditions along this axis, using reasonably stiff surfaces to bound the cell, to determine the effect this would have. A comparison of the time dependence, Fig. 8, demonstrates that the effect of the cyclic boundary is surprisingly small, although the simulations with bounding surfaces should be more representative of magnetic systems.

Thermal coarsening. Simulation results were obtained for 10 and 30 vol. % suspensions at dimensionless temperatures ranging from $J = 0.1$ to 0.325. The magnitude of these thermal fluctuations and their effect on the optical transmittance can be seen in the 10 vol. % structures in Fig. 9, which shows z-axis views for samples structured for 75 ms. The time evolution of the optical attenuation length and transmittance for selected values of J is shown in Fig. 10 for the same volume fraction. The change in the attenuation length over this temperature range is significant, roughly a factor of 6 at 150 ms, decreasing from ~130 ball diameters at $J = 0.100$ to less than 20 at $J = 0.325$. A detailed analysis of these simulation data show that for $J \geqslant 0.275$, the thermal fluctuations are large enough that only a fluctuating chain phase exists, that does not coarsen into crystalline domains. Thus the optical attenuation length plateaus at some small value.

Annealing. We have seen that thermal fluctuations can decrease the optical transmittance, but thermal fluctuations of the proper magnitude can also be used to increase the optical transmittance, by preventing particles from becoming

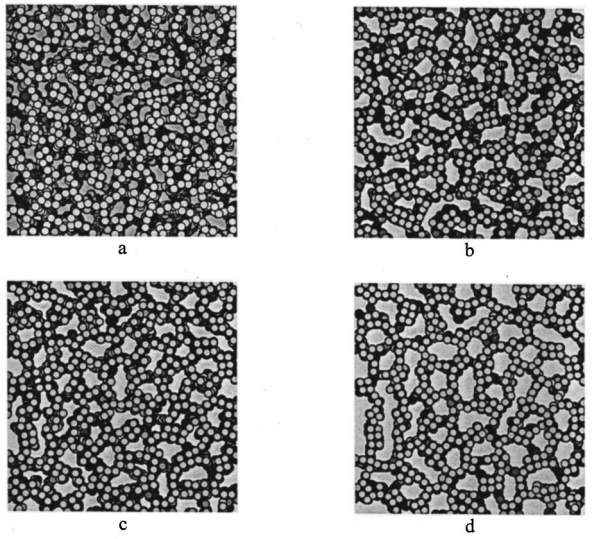

FIG. 11. Effect of annealing on the optical transmittance. Views of a simulated 30 vol. % suspension parallel to the applied field for (a) an athermal simulation after 150 ms; (b) a 75 ms ramped anneal; (c) a sample annealed at $J=0.200$ for 150 ms; and (d) the structure in (c) after a quench to $J=0$ for 10 additional ms.

stuck in local potential wells. To quantify this effect, two types of annealing simulations were run: ramped anneals, in which the force ratio J was linearly decreased from 0.35 to 0 over a time of 75 ms and fixed anneals, where J was held at a fixed temperature for 150 ms and then quenched to $J=0$ for an additional 10 ms. The optical attenuation lengths are significantly increased by these procedures relative to those obtained athermally.

Ramped anneals. The increased order obtained in ramped anneals is appreciated by comparing the 30 vol. % athermal structure in Fig. 11(a) to the annealed structure in Fig. 11(b). The effect this order has on the optical attenuation length and transmittance is shown in Fig. 12 for concentrations from 10–50 vol. %. The percentage increase in the attenuation length at 75 ms relative to the athermal results ranges from ~38% for $\phi=10$ vol. % to 100% for $\phi=50$ vol. %, indicating a substantial increase in order. Of course, this will have a marked effect on the transmittance, especially when the sample thickness is greater than the optical attenuation length.

Fixed anneals. The results obtained by fixed temperature anneals were even more dramatic, as exemplified by a comparison of Figs. 11(c) and 11(d) to the athermal structure in Fig. 11(a). Figure 11(c) is a fixed $J=0.200$ anneal after 150 ms and Fig. 11(d) shows this structure after quenching to $J=0$ for 10 ms. The computed optical attenuation length and transmittance is shown in Fig. 13 for samples that were annealed at the dimensionless temperatures $J=0.100$, 0.200, 0.225, 0.250, 0.275, 0.300, and 0.325, at $\phi=10$ vol. %. The sudden increase in the optical attenuation length after the quench to zero temperature is especially pronounced for $J=0.200$ where a final attenuation length of 184 particle diameters was obtained. This is a 57% increase over the athermal case, where an attenuation length of 117 particle diameters is expected at 150 ms, based on extrapolating the fit to the 75 ms of simulation data to 150 ms. Under the same fixed annealing conditions, the optical attenuation length increases

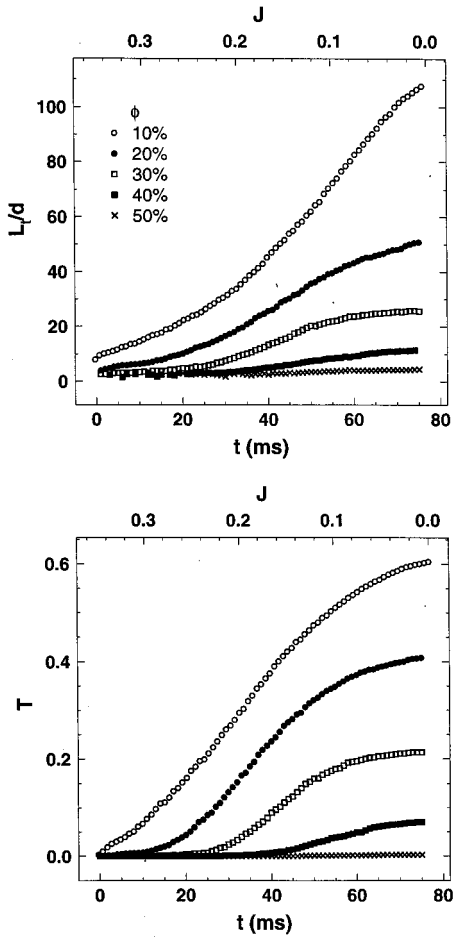

FIG. 12. Optical transmittance and attenuation for simulated ramped anneals at selected concentrations.

by a factor of 4 over the athermal case for $\phi=30$ vol. %.

As J increases to about 0.275, the effect of thermal fluctuations is large enough that significant crystalline order ceases to develop. At these high temperatures only an equilibrium chainlike phase exists, consequently anneals at temperatures greater than this are ineffective. Likewise, for values of J beneath roughly 0.100 the effect of thermal fluctuations on structural development is small, so only a narrow range of J is effective for annealing. In an actual experiment, where the field is the conveniently controlled parameter, one would select the applied field to be very close to that needed to induce chaining.

Switching. It is interesting to investigate whether the induced optical transmittance can be switched rapidly enough to be practical in any applications. The off switching can be passive, via Brownian motion, or the switching can be active, by switching between uniaxial and biaxial fields. The biaxial field is assumed to be a field of constant magnitude rotated in a plane perpendicular to the uniaxial field, but more complex biaxial fields can be considered as well.

Passive switching. When the field is turned off, Brownian motion can play an important role in reducing the optical transmittance. The results of a simulation of this passive off switching is shown in Fig. 14. The field is applied at 0 ms, and the transmittance progressively increases for the next 150 ms, until the field is turned off, at which point diffusion

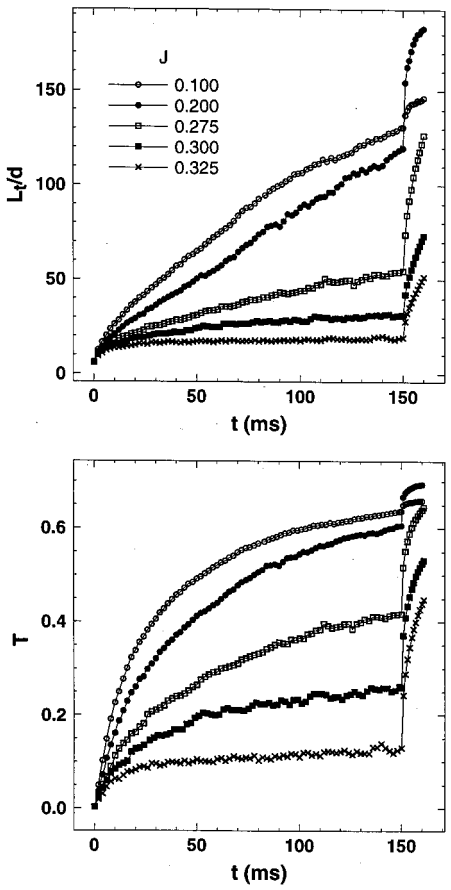

FIG. 13. Optical transmittance and attenuation for simulations of a 10 vol. % suspension quenched at fixed J. At 150 ms J was reduced to zero, causing a rapid increase in the transmittance, especially for the $J=0.200$ case.

reduces the optical transmittance. At 160 ms the field is again applied, and because of remnant spatial correlations the transmittance increases much more rapidly than the first time. These remnant correlations are shown in Fig. 15.

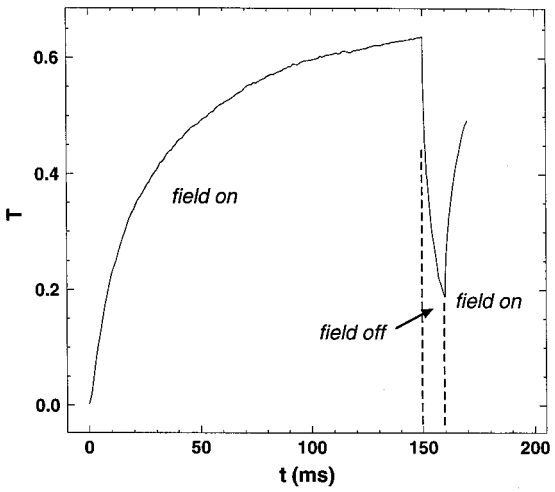

FIG. 14. Simulated passive off-switching for a 10 vol. % suspension. In the first 150 ms $J=0$, then $J=0.325$ for 10 ms, then $J=0$ again.

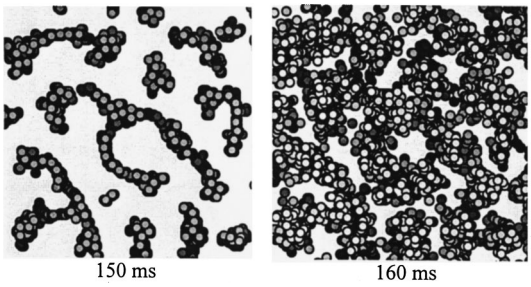

FIG. 15. Field-axis views of passive off-switching structures. The figure on the left is after 150 ms of coarsening, and on the right, after Brownian motion was allowed to destructure the sample for 10 ms.

Active switching. The switching behavior can be much more rapid for large particles when the field is switched between uniaxial and biaxial, rather than merely being switched on and off. Figures 16 and 17 show these results. Note that the onset of transmittance is slow compared to the off-switching time scale, which is of the order of 1 ms. The practical disadvantage of using this technique is that multiple electrodes or coils would have to be used. Active switching is simply not required for suspensions of small magnetic particles, as diffusion is quite fast enough, as discussed below. This reversibility indicates that field-structured materials may prove practical as optical switching devices, or sensors for magnetic fields.

EXPERIMENTAL RESULTS

Typical results for the experimental field-induced optical transmittance are shown Fig. 18 for a sample of 1.0 wt. % (~0.2 vol. %) Fe_3O_4 exposed to a magnetic inductance field of $B=5.2\times10^{-3}$ T. The field was turned on for just over 30 min, turned off for 7 min, and turned back on. Several interesting features can be observed in this transmittance graph. First, immediately after turning on the field the transmittance

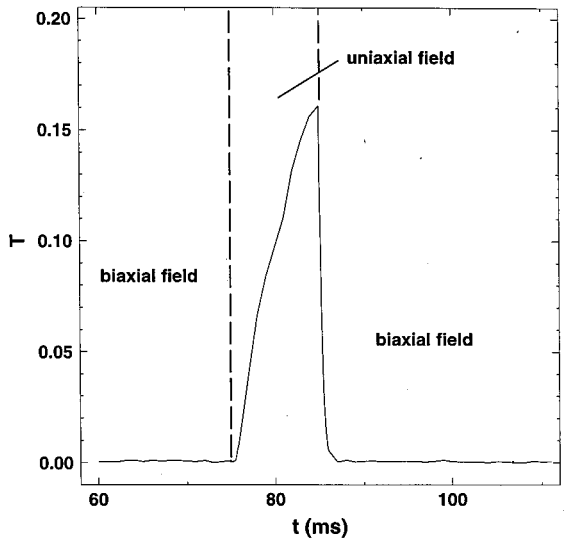

FIG. 16. Simulated active-switching for a 10 vol. % suspension. The onset of transmittance is slow compared to the off-switching time scale of ~1 ms.

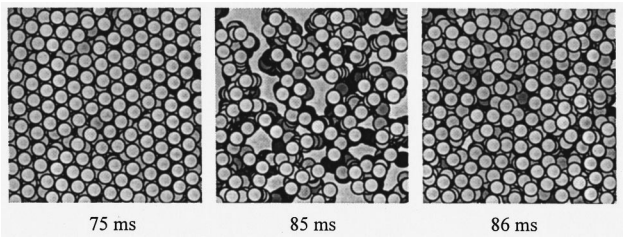

FIG. 17. Field-axis views of active switching structures. The sample was structured for 75 ms in a biaxial field, at which time the field was switched to uniaxial for 10 ms, then the field was switched to biaxial again for 1 ms.

increases abruptly for a period of a few seconds. The cause of this initial transient is not certain, but it might be due to the long axis of the aspherical particles rotating to align with the field, an explanation supported by the experiments done with spherical Fe particles described below. After this initial transient, the transmittance increases slowly until it approaches a plateau, in a manner similar to that obtained from the simulations, Fig. 14. Second, the drop in the transmittance is very rapid, and when the field is turned on again the transmittance increases much more rapidly than initially, presumably due to residual spatial correlations in the suspension. These effects are in good qualitative agreement with the simulations, except that the initial transient is not seen in simulations of spherical particles.

A quantitative analysis of the experimental and simulation data elucidates some problems. As mentioned, athermal simulations at low particle volume fractions (10%) indicate a coarsening exponent of $\beta \cong 0.55$, and a plateau transmittance of $T_\infty = 0.81$. Fitting the first 30 min of the experimental data in Fig. 18 gives $T_\infty = 0.35$ and $\beta = 0.70$, Fig. 19, and a fit that is satisfactory after the initial jump in transmittance. Thus a power-law increase in the optical attenuation length is obtained, with an exponent β that is in reasonable agreement with simulation, but the experimental plateau transmittance T_∞ is unexpectedly small. If the equilibrium state is bct columns, which have a packing fraction of $\phi_c \cong 0.6981$, one would expect the transmittance to approach $T_\infty = 1 - \phi/\phi_c$, neglecting surface effects due to the finite column diameter. For the simulated field-structured material at 10 vol. %, T_∞ should be approximately 0.86, which is close to the value of 0.81 obtained in the fit to these data. On the other hand, for the experiment run at 0.2 vol. %, T_∞ should be essentially 1.00. Instead, it is roughly $\frac{1}{3}$ that value, indicating unexpected disorder in the experimental structures.

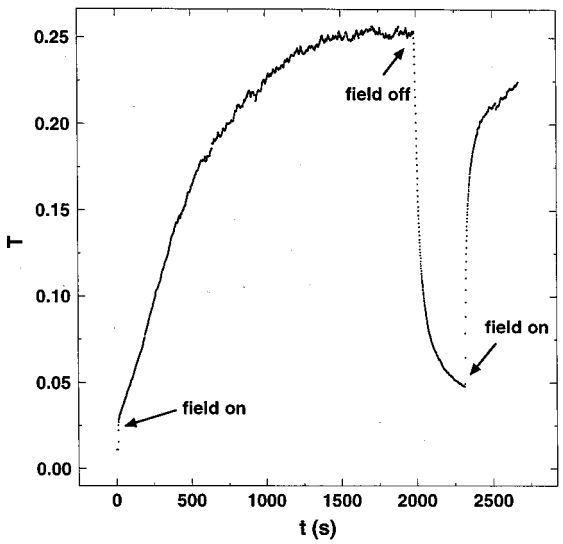

FIG. 18. Optical transmittance of a system of 0.2 vol. % Fe_3O_4 particles in a 5.2×10^{-3} T field.

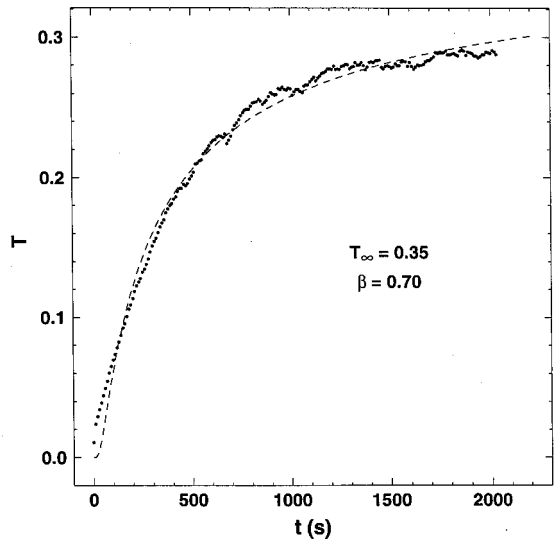

FIG. 19. Fit to the initial transmittance rise of the data in Fig. 18.

Concentration dependence. The extent of the disagreement between simulation and experiment is revealed in a study of the concentration dependence of the transmittance. Fe_3O_4 dispersions in the range of 0.2–0.8 vol. % were structured in a fixed magnetic field of $B = 5.2 \times 10^{-3}$ T, to obtain the results in Fig. 20. The transmittance T was again fit to the form $T = T_\infty / \exp(\tau/t)^\beta$, but in order to investigate the plateau in the transmittance systematically, we fixed the exponent β to 0.5, which is roughly the expected value at such low concentrations. Ideally, we would have floated all of the fit parameters, but this gives unstable results at the higher concentrations. The fitting parameters T_∞ and τ are given in Table II.

The experimental data show a precipitous drop in the asymptotic transmittance with increasing particle concentration. A comparison of the concentration dependence of the experimental and simulation values of T_∞ is shown in Fig. 21. Although the simulations and experiments both show a substantial decrease with concentration, the experimental value of T_∞ drops to an exceedingly small value at a volume fraction of only 1.0 wt. %. This indicates that our experimental system contains a source of disorder that is not in the athermal simulations. One obvious source of disorder is thermal fluctuations, and another is that interparticle friction pins coarsening.

The time scale for the structural coarsening seems to increase with increasing concentration, but this parameter is relatively noisy. The experimental values for the time scale are longer than those from the simulations, in part because the 300 cp viscosity of the suspending fluid is much larger than the 1 cp used to determine the timescale in the simula-

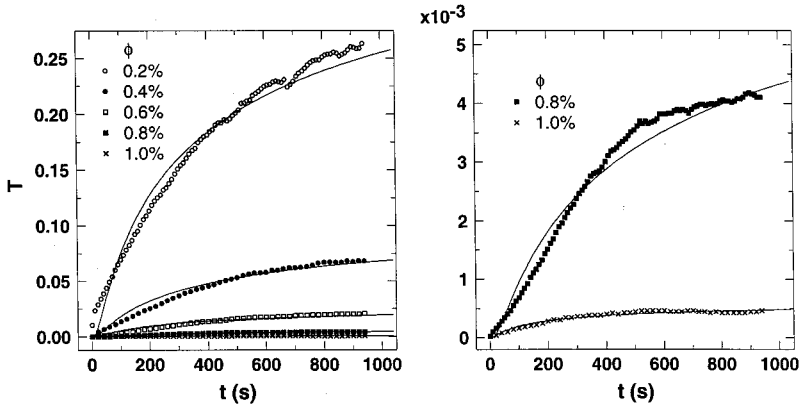

FIG. 20. Optical transmittance for selected concentrations of Fe_3O_4 at an applied field of 5.2×10^{-3} T. In the right hand graph the ordinate is expanded for the high concentration samples. The fit parameters are in Table II.

tion, but also because this timescale is dependent on the square of the system size (for $\beta=\frac{1}{2}$), which for the simulations is no larger than 37 particle diameters, and for the experimental system is ~1500 particle diameters.

Thermal fluctuations. In simulations we have seen that thermal fluctuations can significantly decrease the optical transmittance. In these simulations the important parameter is the ratio of the Brownian force to the dipolar force $J \propto k_B T/B^2$. Because J is inversely proportional to the square of the magnetic field, it is convenient to explore the effect of Brownian motion experimentally by changing the magnetic field.

Experimental transmittance measurements on solutions of 0.2 and 0.4 vol. % Fe_3O_4 in magnetic inductance fields from $B=3.0-6.0\times10^{-3}$ T, representing a fourfold change in J, yield results that are qualitatively similar to the simulations. Transmittance results are presented in Fig. 22 for the 0.2 vol. % Fe_3O_4 suspension. The data are much too noisy to extract the exponent β, so we merely attempted to estimate the plateau transmittance T_∞ by fitting with β fixed at 0.5. An increase of a factor of 2 in the plateau transmittance is found, indicating that we are in a field regime where thermal fluctuations can play a role.

The dependence of the plateau transmittance T_∞ on the applied field is presented for both simulation and experiment in Fig. 23. In both cases T_∞ increases with increasing field (or decreasing temperature). The effective field reached through simulations is apparently larger than that reached by experiment, as the value of T_∞ levels off at high fields, where it approaches the expected value for bct packing, $T_\infty=1-\phi/\phi_c$, for the 10 vol. % sample, and a somewhat smaller value for the 30 vol. % sample. Unfortunately, in experiments with our open solenoid we could not reach sufficiently large fields to find the asymptotic field regime, due to excessive coil heating. However, over the experimentally accessible field regime thermal fluctuations clearly play a role in increasing disorder and thus reducing the optical transmittance in field structured materials. On the other hand, direct microscopic examination of particle chain formation indicate that particle roughness might also lead to increased disorder in the system, as will be explained below.

Particle roughness and friction. The effect of particle roughness is not often addressed in the fields of electrorheology and magnetorheology, primarily because the effects are not easily understood theoretically or experimentally. One would expect particle roughness to increase the disorder in a field structured system by pinning structures into local energy minima, thus reducing the optical transmittance drastically from the expected value. The effect is analogous to quenching certain two-component polymer-solvent mixtures into the spinodal part of the two-phase region. Phase separation and coarsening will occur unless the concentration of polymer in the polymer-rich component exceeds the concentration where it becomes glassy, at which point spinodal decomposition effectively halts, due to the extremely large monomeric friction factor. This is actually one method for manufacturing microporous filters, and is an example of pinning due to the large concentration fluctuations that can occur during phase separation. Similar pinning might also occur in field structured materials, due to the importance of interparticle friction and roughness in the high concentration columnar regimes.

To obtain some appreciation of the effect of particle roughness, consider a single rough particle in contact with a smooth wall, and subjected to a tangential force $\mathbf{F}_t$ parallel to the wall, and a radial force $\mathbf{F}_r$ perpendicular to the wall, both of which act on the particle center of mass, Fig. 24. (We recall that particles interacting via dipolar potentials are subject both radial and tangential forces.) This is a simplification of a rough particle interacting with a second, enchained rough particle, but is sufficient to illustrate the point. The particle has a static coefficient of friction c with the wall, and has an asperity that contacts the wall at a point whose vector to the center of mass forms an angle θ to the surface of the wall. There are two possible modes of motion of the particle; it can slide along the surface, or roll along the surface. To slide along the surface, the tangential force must exceed the force of friction, i.e., $\mathbf{F}_t \geqslant c\mathbf{F}_r$. To roll along the surface, one can readily show that $\mathbf{F}_t \geqslant \mathbf{F}_r c \tan\theta$. Thus if $c\tan\theta < c$, the particle will roll when $\mathbf{F}_t \geqslant \mathbf{F}_r c\tan\theta$, and if $c\tan\theta > c$, the

TABLE II. Optical transmittance fitting parameters for experimental structures. (The exponent β was held constant at 0.5 in these fits.)

ϕ	T_∞	τ
0.002	0.45	322
0.004	0.13	371
0.006	0.035	340
0.008	0.0087	497
0.1	(0.00073)	(173)

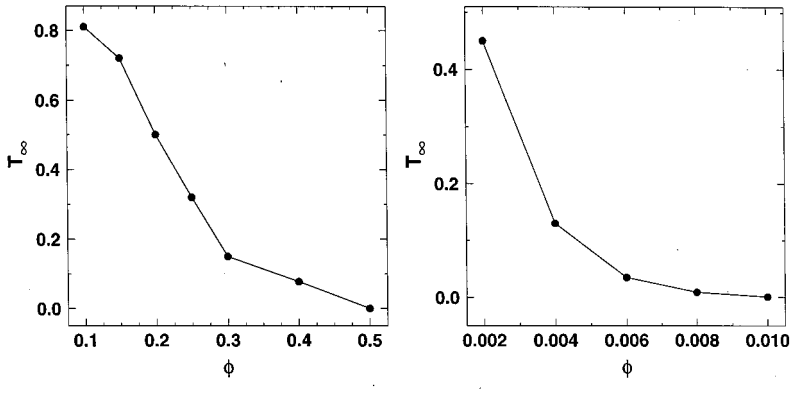

FIG. 21. The plateau transmittance T_∞ of experimental and simulated structures is compared. Note the difference in concentration ranges.

particle will slide when $\mathbf{F}_t \geqslant c\mathbf{F}_r$. In either case, there is a finite force threshold for motion; as long as the coefficient of friction is finite there is a threshold for sliding; and if the particle is rough there is a threshold for rolling (for a spherical particle $\theta = 90°$ and $c \tan\theta = 0$).

What effect might these barriers to motion have on structuring? First, we note that in general the radial and tangential components of the force scale with field in the same fashion, indicating that there might not be a field dependence, as long as the dipolar forces effectively dominate the Brownian force. Second, large interparticle friction and/or surface roughness will lead to situations where further structural development is not possible—which is a form of pinning. This is possibly the effect we are observing.

Pinning or thermal fluctuations? The effects of pinning and thermal fluctuations can be distinguished experimentally. First, the effect of pinning should be independent of the field as long as the dipolar forces dominate the Brownian force. Thus if pinning has locked the structures into a local energy minimum with sufficient disorder to reduce the optical transmittance, increasing the field should not increase the transmittance. Likewise, if field has been increased beyond this point, a small reduction of the field should not decrease the transmittance.

If thermal fluctuations are the dominant source of disorder, increasing the field will increase the plateau transmittance T_∞ and decreasing the field will decrease T_∞. By structuring a suspension in a reasonably large applied field, and allowing the suspension to reach its plateau transmittance, we can determine the field at which thermal fluctuations become an important source of disorder by decreasing the field until the optical transmittance starts to decrease. In the field regime where there is no decrease in the transmittance, the disorder is evidently due to pinning.

To investigate this effect, a 0.2 vol. % suspension of Fe_3O_4 particles was placed in a relatively large $B = 7.8\times10^{-3}$ T structuring field until the transmittance had reached a plateau. The field was then stepwise decreased and the optical transmittance monitored. The transmittance was not affected until the field was reduced to 2.6×10^{-3} T. Beneath this field, the transmittance decreased in a stepwise fashion with the field. These results provide convincing evidence that pinning is important in the coarsening kinetics of field structured suspensions consisting of rough particles.

The issue of pinning can be further investigated by examining the field-induced optical transmittance of suspensions of smooth, spherical particles. If such suspensions show greater optical transmittance then this argues that pinning is indeed affecting structure formation. We obtained roughly spherical 1–3 μm carbonyl Fe particles from Lord Corporation. Due to the increased size of these particles, compared to the Fe_3O_4 particles, sedimentation occurred at lower magnetic fields, so we were restricted to runs at high fields, and here we found the transmittance to be much greater than for the Fe_3O_4 particles. Results for a 2.5 vol. % suspension subjected to a 5.2×10^{-3} T field are shown in Fig. 25. The field was on for approximately 53 min, then off for approximately 1 min, and then turned back on. By comparison, roughly the same plateau transmittance, and thus attenuation length, is obtained for a 0.4 vol. % suspension of Fe_3O_4 particles, Fig. 26. At a volume fraction of 0.6% Fe_3O_4 essentially no light is transmitted. In each case the transmittance is not as great as expected, but the large variation in the plateau transmittance demonstrates that pinning due to particle roughness is playing an important role.

Some additional details concerning structure formation in

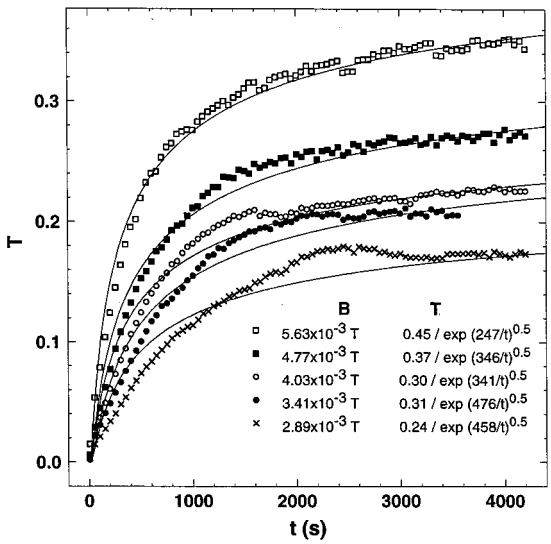

FIG. 22. The evolution of the optical transmittance for a 0.2 vol. % suspension at selected magnetic fields. The time scale of structure formation is not merely proportional to the square of the field, indicating the importance of thermal fluctuations.

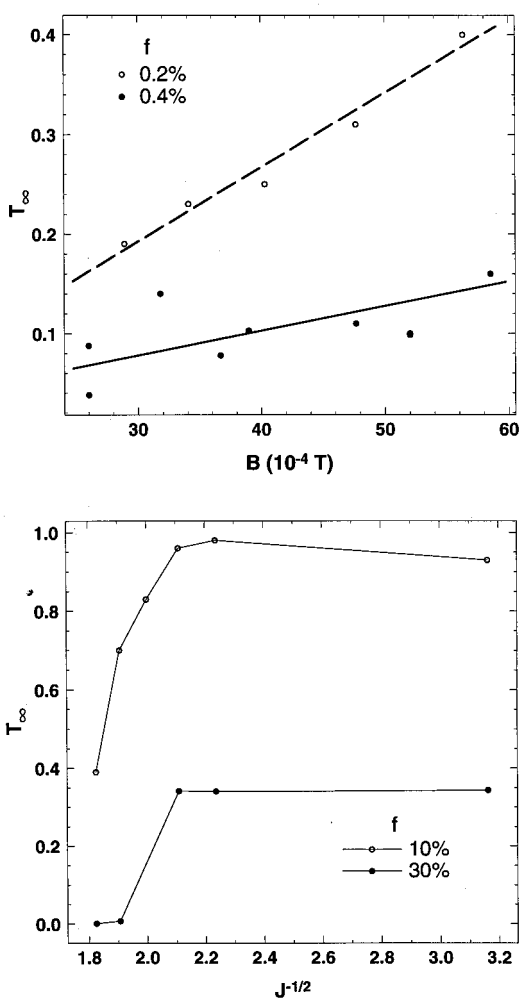

FIG. 23. The dependence of the plateau transmittance T_∞ on the applied field. The poor agreement is probably due to the importance of particle roughness and friction in the experimental system.

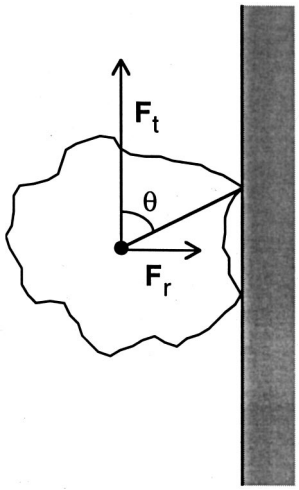

FIG. 24. Schematic of a rough particle against a smooth surface with applied forces parallel and perpendicular to the surface acting on its center of mass.

these particle suspensions is shown in Fig. 27. In Fig. 27(a) is shown the initial increase in transmittance for each suspension. As mentioned previously, the transmittance of the 0.4 vol. % suspension of Fe_3O_4 particles initially rises rapidly, but there is no such transient for the Fe spheres. Previously we suggested that this sudden change in the data for the Fe_3O_4 particles may be due to the initial rotation of the irregularly shaped particles to align with the field, but as the initial rise for both is nearly identical, it may be indication that the effects of pinning in the aspherical particles occur very early in the run, almost immediately suddenly slowing the rate of growth. Figure 27(b) shows the behavior in transmittance immediately after the field was turned off for both experiments, further evidence that pinning may play a role for the aspherical particles. The transmittance for the spheres also drops much more quickly than for the aspherical particles. Pinning might again be the cause for this difference, slowing the relaxation for the Fe_3O_4 particles, but the issue is actually complicated, because of the residual magnetization of the particles causing appreciable contact interactions.

Annealing. Ramped annealing was examined experimentally, by steadily increasing the magnetic field at ambient temperature, using suspensions of the Fe spheres described above. Figure 28 shows a comparison of the optical transmittance of a ramped anneal and a deep quench at a fixed magnetic field of 5.2×10^{-3} T—effectively in the athermal limit. In the ramped anneal we began with an applied field of $\sim3.05\times10^{-3}$ T and increased this by 0.43×10^{-3} T every minute during the first 300 s of the experiment, for a final constant field of 5.2×10^{-3} T. After 2800 sec the deeply quenched sample transmitted just under 12% of the light, whereas the ramped anneal transmitted almost 17% of the light. Thus the optical attenuation length of the ramped annealed sample is 20% greater than the deep quench, in good agreement with simulation results.

DISCUSSION

We have shown that a number of factors are important in the coarsening dynamics of field structured materials. These factors include the expected effect of the strength of the magnetic field, the liquid viscosity, and the sometimes competing influence of thermal fluctuations, but also the unexpected effect of particle friction, and the strong dependence on particle concentration. Both experiments and simulations show that thermal fluctuations can both reduce the transmittance, when the stochastic force dominates the dipolar forces, and increase the optical transmittance, by annealing away defect structures, when the thermal force is comparable to the dipolar force. The effect of particle friction is actually quite large, causing the expected plateau transmittance to be much smaller than expected from simulation, by pinning structures into local energy minima. This effect has not be accounted for in any models of electrorheology or magnetorheology, but might be important in increasing the stress of sheared-induced dipolar fluids. Accounting for particle friction would make simulations very difficult, and perhaps it would no longer be possible to run systems large enough to examine the optical attenuation length.

The experimental measurements also demonstrate the power law coarsening which is observed in the simulations and is predicted by theory, which seems surprising in light of the pinning effects. In the simulations we attribute the coars-

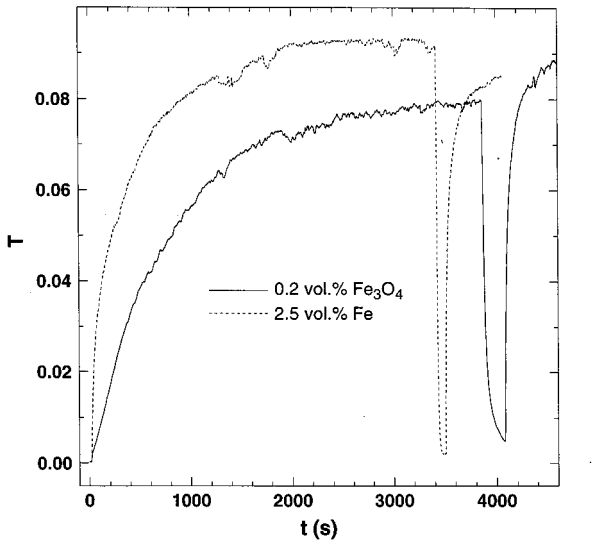

FIG. 25. Optical transmittances of 2.5 vol. % Fe particles and 0.2 vol. % Fe_3O_4 particles subjected to a 5.2×10^{-3} T inductance field. A fit to the Fe data gives a coarsening exponent of $\beta=0.45$.

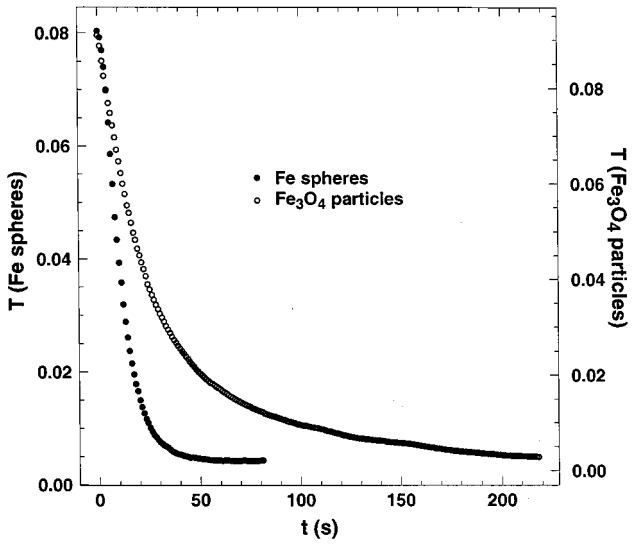

FIG. 27. The passive off-switching dynamics of the 2.5 vol. % Fe particles and 0.2 vol. % Fe_3O_4 particles is compared. Surprisingly, the off-switching is faster for the larger particles, which might be due to the smaller magnetic remnance of Fe.

ening to dipolar interactions that occur because of defect structures. We have not been able to find experimental or simulation conditions that clearly demonstrate the occurrence of defect free chains that might coarsen due to thermal fluctuations.

Finally, our experiments show that the field-induced optical transmittance is reversible, prompting us to consider the possibility for applications. We recall that Brownian motion rapidly drops the transmittance when the field is reduced, but remnant spatial correlations remain, so the transmittance increases relatively rapidly when the field is turned on again. The experimental time scales are quite long, but reasonable response times could be achieved in a normally on device consisting of nanoscale particles suspended in a low viscosity liquid at high applied fields. (Nanoparticles would no longer be in the simple geometrical optics limit, so such a device would have to be calibrated.) For example, to obtain a reasonable increase in the transmittance after destructuring, took about 50 s with an applied field of 5.0×10^{-3} T and in a viscosity of 300 cp. Decreasing the viscosity to that of a short chain hydrocarbon, $\sim$1 cp, and increasing the applied field to 0.500 T would give a characteristic time of $\sim$1 ms for structuring, a timescale that should be independent of

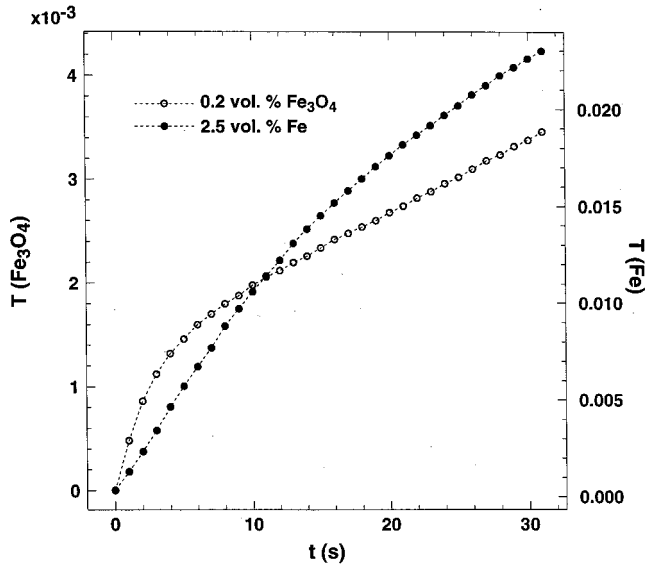

FIG. 26. An expanded view of the initial increase in the optical transmittance of the data in Figs. 25, shows that only the aspherical particles show an initial rapid increase in the transmittance, indicating that this effect is due to particle rotation.

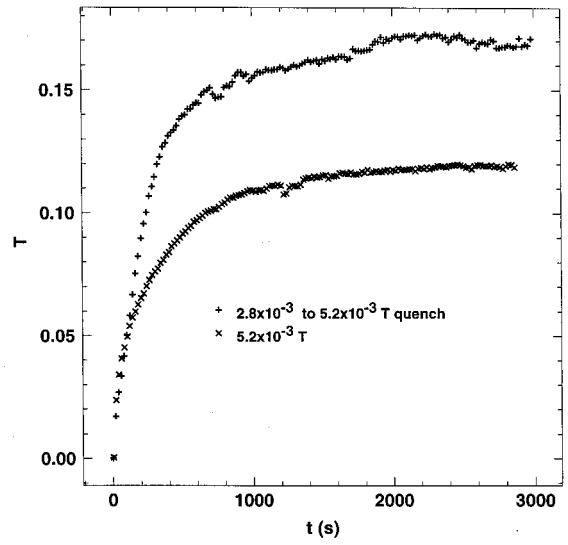

FIG. 28. Graph of the optical transmittance for two experiments, one, where the magnetic field was held constant at approximately 5.2×10^{-3} T, and the other where the magnetic field was increased from approximately 3.0×10^{-3} to 5.2×10^{-3} T over the first 5 min and held at 5.2×10^{-3} T for the remainder of the experiment.

particle size. The destructuring time, under Brownian motion, will scale as the time it takes a particle to diffuse its own radius $R^2/D_t \sim R^3$, a time scale proportional to the reciprocal rotational diffusion constant. Thus if we reduce the particle size from ~ 1 μm to 10 nm, and reduce the viscosity to 1 cp, the destructuring time will decrease from ~ 50 s to ~ 0.1 μs. Note that the characteristic times for structuring and destructuring are quite different; structuring scales as the field squared [3] and is independent of particle size, and destructuring scales as the cube of the particle size. Furthermore, if the thickness of the sample is decreased in the direction of the field, the time scale of transmittance will be greatly reduced, since this timescale goes as roughly the square of the thickness.

The rapid reversibility of the induced transmittance with small Brownian particles, perhaps nanoclusters of gadolinium, makes the use of this effect for optical-fiber-based magnetic field sensors a possibility. Such devices would be extremely sensitive to the field direction and homogeneity and would be useful in measuring fields, and thus currents, in a safe (wireless) fashion near high tension power lines. We have observed that over a certain range of $J \propto k_B T/B^2 a^3$ the plateau transmittance is sensitive to J. Thus if it is desired to detect large fields the particle size can be decreased, and vice versa. Multiple cells containing different size particles could span a large range of fields, or the timescale of structuring could be used to determine the field.

CONCLUSIONS

We have presented a simulation and experimental investigation of the optical transmittance that can be induced in a suspension of magnetic particles by a magnetic field. The studies demonstrate that a number of factors are important in the coarsening dynamics of field structured materials, with temperature and particle friction playing important and sometimes complex roles, with temperature sometimes increasing or decreasing the transmittance. Particle friction is actually quite important, causing the expected plateau transmittance to be much smaller than expected from simulations of smooth spheres, by pinning structures into local energy minima. A complete model of electrorheology or magnetorheology will have to consider such effects.

The experimental measurements also demonstrate the power law coarsening which is observed in the simulations and predicted by the thermal coarsening theory. In the simulations we attribute the coarsening to dipolar interactions that occur because of defect structures. We have not been able to find experimental or simulation conditions that clearly demonstrate the occurrence of defect-free chains that might coarsen due to thermal fluctuations. Finally, it was found that the field-induced optical transmittance is reversible and might find applications as optical switching devices, with either passive or active switching.

ACKNOWLEDGMENTS

Sandia is a multiprogram laboratory operated by the Sandia Corporation, a Lockheed Martin Company, for the U.S. Department of Energy under Contract No. DE-AC04-94AL8500. This work was supported by the Division of Materials Sciences, Office of Basic Energy Sciences, U.S. Department of Energy (DOE).

[1] See the many excellent articles in *Proceedings of the 5th International Conference on Electro-rheological Fluids, Magneto-rheological Suspensions and Associated Technology*, edited by W. A. Bullough (World Scientific, Singapore, 1996).
[2] A. P. Gast and C. F. Zukoski, Adv. Colloid Interface Sci. **30**, 153 (1988).
[3] J. E. Martin, R. A. Anderson, and C. P. Tigges, J. Chem. Phys. **108**, 3765 (1998).
[4] J. E. Martin, J. Odinek, and T. C. Halsey, Phys. Rev. Lett. **69**, 1524 (1992); J. E. Martin, J. Odinek, T. C. Halsey, and R. Kamien, Phys. Rev. E **57**, 756 (1998).
[5] J. E. Martin, R. A. Anderson, and C. P. Tigges, J. Chem. Phys. **108**, 7887 (1998).
[6] J. P. Wilcoxon, S. A. Craft, and T. R. Thurston, Rev. Sci. Instrum. **67**, 3021 (1996).
[7] J. P. Wilcoxon, J. E. Martin, and J. Odinek, Phys. Rev. Lett. **75**, 1558 (1995).
[8] J. Lui, E. M. Lawrence, M. L. Ivey, G. A. Flores, J. Bibette, and J. Richard, in *Electrorheological Fluids: Mechanisms, Properties, Technology and Applications*, edited by R. Tao and G. D. Roy (World Scientific, Singapore, 1994), p. 172.
[9] J. M. Ginder, Phys. Rev. E **47**, 3418 (1993).
[10] S. Cutillas, A. Meunier, E. LeMaire, G. Bossis, and J. Persello, in *Proceedings of the 5th International Conference on Electrorheological Fluids, Magneto-rheological Suspensions and Associated Technology* (Ref. [1]), p. 270.
[11] C. M. Cerda, R. T. Foister, and S. G. Mason, J. Colloid Interface Sci. **82**, 577 (1981).
[12] T. C. Jordan and M. T. Shaw, in *Proceedings of the 2nd International Conference on Electrorheological Fluids*, edited by J. D. Carlson, A. F. Sprecher, and H. Conrad (Technomic, Lancaster, PA, 1990), p. 231.
[13] M. Gross (unpublished).
[14] T. C. Halsey and W. Toor, Phys. Rev. Lett. **65**, 2820 (1990); J. Stat. Phys. **61**, 1257 (1990).
[15] J. R. Reitz and F. J. Milford, *Foundations of Electromagnetic Theory* (Addison Wesley, Reading, MA, 1967), pp. 210–214.
[16] J. R. Reitz and F. J. Milford, *Foundations of Electromagnetic Theory* (Ref. [15]), pp. 98–101.
[17] B. J. Berne and R. Pecora, *Dynamic Light Scattering* (Wiley, New York, 1976), pp. 83–86.
[18] L. Landau and E. M. Lifshitz, *Statistical Physics*, 2nd ed. (Pergamon, Oxford, 1984), p. 192ff.
[19] H. X. Guo, Z. H. Mai, and H. H. Tian, Phys. Rev. E **53**, 3823 (1996).
[20] G. L. Gulley and R. Tao, Phys. Rev. E **56**, 4328 (1997).